NANO LETTERS

2003
Vol. 3, No. 4
485−491

Local Refractive Index Dependence of Plasmon Resonance Spectra from Individual Nanoparticles

Jack J. Mock,* David R. Smith, and Sheldon Schultz

Department of Physics, University of California, San Diego, La Jolla, California 92093-0319

Received January 24, 2003; Revised Manuscript Received February 25, 2003

ABSTRACT

We present an experimental optical darkfield microscope study of the dependence of the plasmon resonance spectrum of individual silver nanoparticles on the local index of refraction. We systematically characterize the position of the resonance peaks associated with the same set of individual silver nanoparticles embedded sequentially in index oils with increasing refractive index. This technique effectively allows the local refractive index to be stepped in increments of 0.04. As the local index is increased, the spectrum from each of the nanoparticles generally undergoes a very regular and reproducible red shift; however, we find that the amount of red shift per index increase varies depending on the shape of the nanoparticle and the mode of excitation. In particular, we find that the spectral peak that occurs in triangular nanoparticles exhibits a noticeably larger red shift than that associated with the dipole mode corresponding to spherical nanoparticles. Our results are consistent with experiments performed on ensembles of similar nanoparticles and suggest that individual nanoparticles may be utilized in biosensing applications where currently ensembles are being investigated.

The exceptional optical properties of surface plasmons—coupled electronic and electromagnetic excitations—are increasingly being appreciated for their potential application to highly efficient and miniaturized optical devices.[1−5] There has been considerable interest recently in gold and silver plasmon resonant structures, made by colloidal chemistry[6−11] or lithographic techniques,[12,13] for their fascinating optical properties, and potential biological labeling and diagnostic applications.[14,15] One example of a device based on the excitation of surface plasmons is the film surface plasmon resonance (SPR) biosensor,[16] in which the optical scattering from a thin gold or silver film is used as a sensitive indicator of the changes in refractive index due to molecular surface binding events. The SPR biosensor achieves its highest sensitivity at the wavelength and angle of incidence condition where coupling of the incident light to local surface plasmon modes in the metallic film is substantial and changes rapidly with molecular binding. Commercially viable detectors have been produced [Biacore].

Surface plasmon (SP) modes can also be excited in nanoparticles. When the particle size (typically 40−120 nm diameter) is significantly smaller than a wavelength, a resonance condition can be satisfied, enhancing both the local and scattered fields at wavelengths corresponding to dipolar and multipolar modes. Note that this resonance is very different in origin than that used in the film SPR biosensors. The metallic film in the SPR case is not intrinsically resonant, but rather depends on the excitation of surface plasmons which act as a damping mechanism on a reflected or transmitted optical beam with relatively sharp wavelength and angular dependence, which is highly dependent on the refractive index of the adsorbed molecules. The optical response of gold and silver plasmon resonant particles (PRPs) can also be expected to exhibit significant sensitivity to their local refractive index, but in this case exhibiting a shift in the peak of the elastic scattering resonance. Given their confined volume and enhanced optical response, PRPs offer the possibility of a new class of miniatured biosensors based upon the local index-induced plasmon resonance peak shift.

Since individual plasmon resonant nanoparticles exhibit enhanced scattering behavior, one might expect that the replacement of the thin metallic film by a patterned film of plasmon resonant particles could result in an even higher sensitivity to local index of refraction in SPR biosensing devices. An alternative to the technique of SPR is to engineer films composed of a layer of PRPs. The peak position of the plasmon resonance of the particles is affected by slight changes in the local index in a manner that is similar to, if not more sensitive than, the traditional SPR films.[17−19] Van Duyne et al. have devised a clever nanosphere lithography technique[20−22] for creating an array of triangular shaped nanoparticles, which they suggest may be more sensitive to local index change than the spherical colloidal particles, due

* Corresponding author. E-mail jmock@physics.ucsd.edu

10.1021/nl0340475 CCC: $25.00
Published on Web 03/14/2003

to the particle shape dependence of the plasmon resonance. Van Duyne et al. have made extensive measurements of the plasmon resonance shift on layers of triangular nanoparticles caused by a variety of solvents of differing dielectrics, as well as by binding DNA and protein molecular monolayers to the surfaces. The resulting sensitivity suggests that an ensemble of plasmon resonant nanoparticles can be used as an effective biosensor. These experiments[17−22] utilize a UV/vis spectrophotometer in transmission mode to measure the extinction cross-section, which includes both light that is scattered as well as light that is absorbed by the array of plasmon resonant particles. Conversely, we use a darkfield microscope to measure only the scattered component of light from the plasmon resonant particles. Mie theory calculations indicate that the extinction cross-section is dominated by the scattering cross-section for plasmon resonant nanoparticles in the size range of our study, therefore the results of the two techniques can be directly compared. However, by measuring just the scattered light, signal-to-noise is increased and individual particles can be more easily studied. Here we will present data suggesting that individual PRPs can be characterized and then monitored to detect local dielectric changes, albeit with some sensitivity variation from particle to particle.

Since spectroscopic techniques have been developed that charcaterize individual PRPs,[6−8,12,14,23−25] we are motivated here to study the plasmon resonance peak shifts due to index changes in the neighborhood of individual PRPs. Theory and previous experimental work have shown that the shape of a nanoparticle has a strong influence on its plasmon resonance spectrum, as does the size and composition.[6,7,9−12,21,23,26−28] It follows that the shift of the plasmon resonance spectral peak as a function of the change in the local refractive index may also be different for nanoparticles of different shape.

We present here a controlled study of the plasmon resonance spectrum from individual PRPs, initially produced by colloidal methods and then bound to a SiO_2 on silicon surface, as a function of the refractive index of a covering liquid. Using the darkfield microscope system we have developed to study individual nanoparticles,[6] we first characterize the spectrum from many individual bound nanoparticles selected in a field-of-view, and then measure the spectral changes corresponding to the index of the covering liquid. In this report we employ index oils to systematically vary the local index of the nanoparticles from 1.44 to 1.56. Analogously, one could perform similar experiments, using the plasmon resonance effect to monitor the change of the local index of a single nanoparticle caused by binding a sufficient number of specific molecules to its surface. We have chosen the index oils used both for their availability and for their effect of nearly matching the ∼1.56 dielectric of the SiO_2 (100 nm film) on the silicon wafer to which the particles are bound. Without the index oils, the individual particles are sitting on a dielectric interface in a local configuration which is uncertain and difficult to model, and which we suggest results in significant spectral variations from particle to particle. If, for example, one particle has more of its surface actually in contact with the high dielectric SiO_2 than another identical one, it may have a different shifted resonance after first applying the index oil. We will return to this idea to help explain the variation from particle to particle, in their initial shift from air to 1.44 index oil, that is observed.

The silver colloids were prepared by nucleating silver salts (silver enhancement kit, BBI International) on 5 nm gold nuclei (BBI International). The typical protocol is as follows: 20 μL of 5 nm gold nuclei, 150 μL initiator from the silver enhancement kit, and 80 μL enhancer from the kit are added (in that order) to 20 mL of DDH_2O. The average size of the silver colloid can be controlled by varying the amount of enhancer added to the solution, which takes approximately one minute to reach completion. For this experiment, we chose to make "medium" sized PRPs with an average diameter ∼70 nm. PRPs are immobilized on polylysine-treated silicon wafers (having ∼100 nm SiO_2 top layer which insulates the PRPs from the conductive silicon), at low density, by placing a drop (50−500ul) of the colloidal solution onto the wafer for ∼1 min, followed by a rinse in DDH_2O and ethanol. The polylysine treatment firmly immobilizes the colloidal silver nanoparticles to the substrate surface. We shall refer to particles in this initial state as "air-dried".

The samples are examined by an optical darkfield microscope system modified for single-particle spectroscopy, and we employ a mapping technique similar to that used in a prior publication to correlate the size and shape of individual nanoparticles to their plasmon resonance spectra.[6] All optical imaging is performed with a Nikon Labophot microscope with CF Plan BD 100X, 0.8 numerical-aperture objective lens. To obtain a plasmon resonance curve from individual silver colloids, light from a 100 W Xe source is directed on the sample area by darkfield illumination, and light backscattered by the particles is collected by the objective and directed to an adjustable image plane aperture, which is used to select an individual particle and remove scattered light from other sources in the sample area. An ocular focused on the aperture enables the operator to view and position the (diffraction limited) image from a single colloidal nanoparticle into the center of the aperture (0.2 mm diameter). Light from this single nanoparticle is then passed into a SPEX 270M grating spectrometer using a mirror and focusing lenses, to which a MicroMax CCD camera (Princeton Instruments/Roper Scientific) is mounted for collection. The wavelength dependence of the source, optics, and CCD is removed by normalizing the measured spectrum to that obtained from a broadband light-scattering target (Labsphere, New Hampshire). Before applying the normalization procedure, a spectrum is first collected from a particle, and then from an empty region of the SiO_2 wafer close to that particle's location, but positioned so that the particle is outside of the aperture selected area. This corresponding background substrate spectrum has been subtracted from each particle spectrum in all of the data presented.

To have a reproducible spatial map of the relative locations of the particles on the SiO_2/Si wafer for reanalyzing after an index oil treatment and wash, we employ a motorized

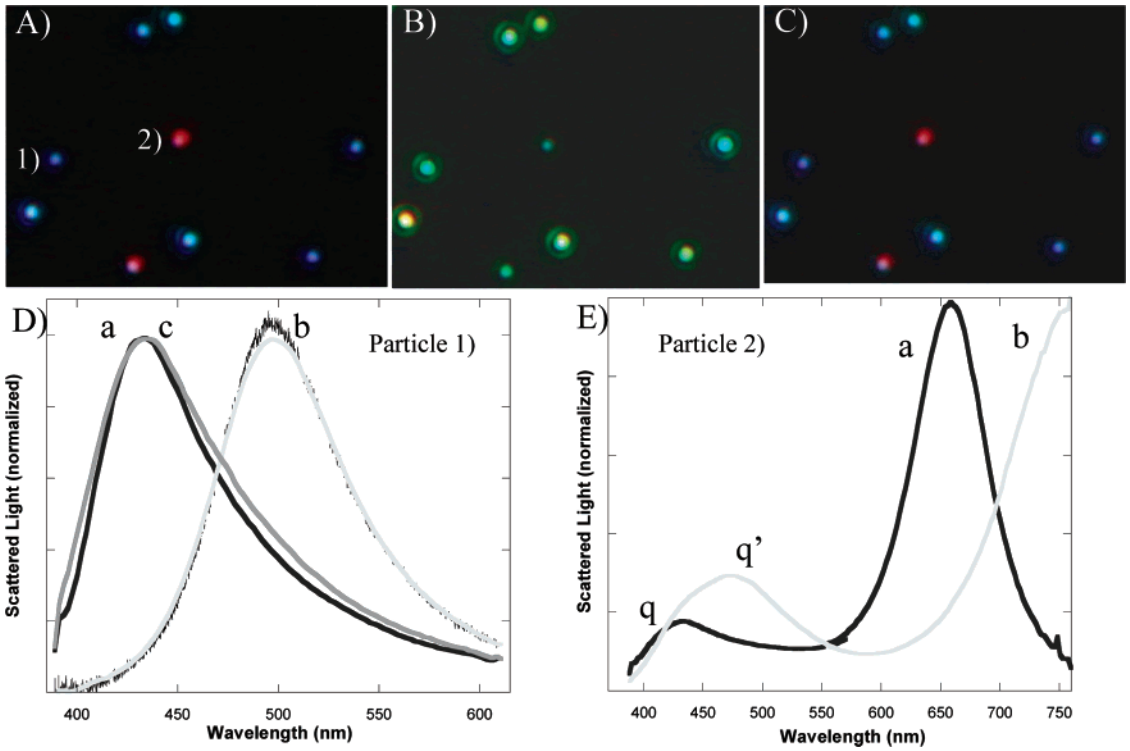

Figure 1. Typical field of silver nanoparticles immobilized on SiO_2 wafer and imaged under darkfield illumination with 100× objective. Color images taken with Nikon Coolpix 995. (A) Before oil. (B) With 1.44 index oil spread over particles. (C) After removal of 1.44 index oil with the described protocol. (D) Spectra taken of an individual blue (roughly spherical) particle (labeled 1): (a) before, (b) during, and (c) after exposure to thin film of 1.44 index oil. Note: We have included the actual pixilated spectral data for the blue particle in oil (b), for comparison with the smoothed curve fits as used for all other spectra in this paper. (E) Spectra taken of typical red (triangle) particle (labeled 2): (a) before and (b) during exposure to thin film of 1.44 index oil. Note the enhancement and shift of the peak q to q′, identified as the quadrupole mode in the text.

stage (Prior) and obtain coordinates of the region of interest using the corner of the wafer as the origin. Then a wide view image containing approximately 100 particles is recorded. This image is subsequently used as a simple pattern recognition template during reanalysis in order to locate and correlate the spectrum of each individual particle to changes of the index oil.

Observing the silver nanoparticles under darkfield illumination, immobilized on a local dielectric interface of air and SiO_2, we see that a typical region contains particles displaying a variety of plasmon resonant colors (Figure 1A). We have determined previously in detailed mapping studies comparing optical and transmission electron microscope images that blue particles (scattering light between ∼400 nm to 480 nm) are roughly spherical (diameters = 40−90 nm), green particles (∼500−550 nm) are typically hexagonal (longest dimension = 60−105 nm), and red particles (∼600−700 nm) have a triangular cross section (longest dimension = 55−120 nm), varying in thickness from platelets to tetrahedrons.[6] Therefore, when we refer to blue particles we consider them to be roughly spherical, and when we refer to red particles we consider them to have a triangular cross section. We have not done electron microscope analysis of the individual nanoparticles used in this study.

We first established the spectra for the selected particles in the air-dried state. Then index oil is applied to the top surface of the SiO_2/Si wafer containing the immobilized nanoparticles. To produce a roughly uniform coating of the oil, a droplet of ∼2 μL in volume is spread (using compressed air) over a 1 cm^2 area. After application of the oil we observe a significant color change in each of the plasmon resonant particles (Figure 1B). The thickness of the oil layer is much greater than the dimensions of any of the nanoparticles and can be considered to form an infinite medium above the SiO_2 surface. Note that particles initially blue in color shift to the green/yellow while particles initially red in color would appear to shift to the blue/green, when comparing Figure 1A and Figure 1B. By rinsing the same sample in xylene for 5 min, then in ethanol for 1 min, and finally blowing dry (with compressed clean air), the oil can be satisfactorily removed from the substrate and the plasmon resonance spectra of the particles shift back to their original color (Figure 1C). A graph showing the initial spectrum (a) and then the red-shifted spectrum (b) of a typical blue (roughly spherical) particle, labeled 1 in Figure 1A, is displayed in Figure 1D. Also shown is the spectrum (c) of that same particle after removal of the spectral shifting oil. From Figure 1B, it would appear that the red (triangular shaped) particle, labeled 2 in Figure 1A, has blue shifted; however, as can be seen from the spectra in Figure 1E, it is evident that the main red plasmon resonance peak (a) of the particle is red-shifted out of the visible spectrum (b), and the apparent shift to the blue green is actually a result of a second peak (q) that is intensified and red shifted into the

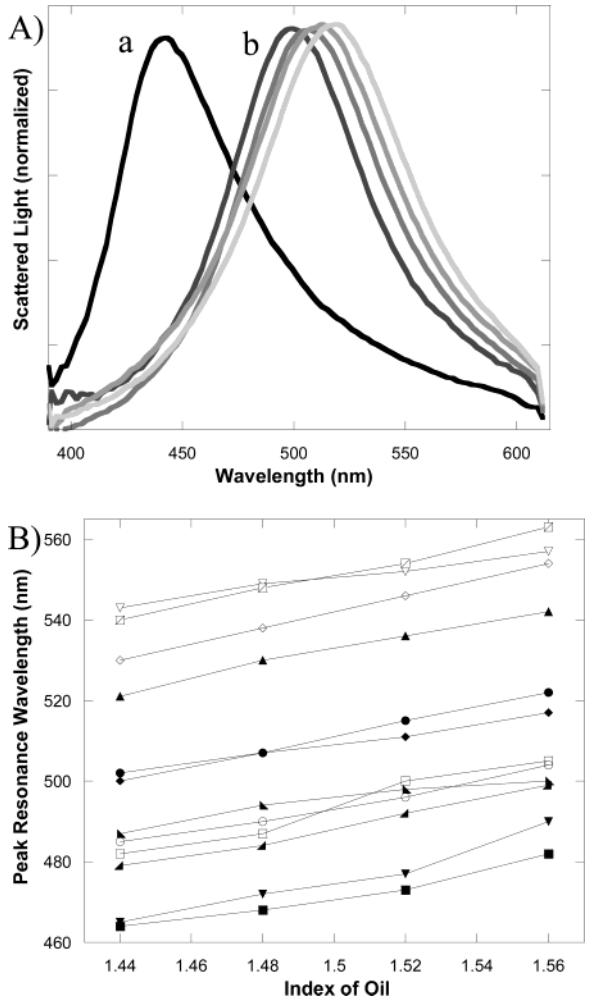

Figure 2. Spectral shift for individual blue (roughly spherical) silver nanoparticles. (A) Typical blue particle spectrum as it is shifted from (a) air to (b) 1.44 index oil, and successive oil treatments in 0.04 index incremental increases. (B) Peak spectral position vs index of oil applied to 12 individual blue (roughly spherical) particles studied. The average slope of the linear fit to these curves suggests a 1.6 nm red shift per 0.01 index increase.

visible spectrum (q′) on addition of the oil. We suggest this second peak corresponds to a quadrupole mode.[27]

Blue (roughly spherical) particles are shifted by an average of 52 nm by spreading a layer of 1.44 index oil over them, based on a mapping of twelve nanoparticles. Note: there is a large deviation (from 21 to 90 nm) from particle to particle for this initial shift. As mentioned earlier, we attribute the variation of this initial shift to the complexity of the actual local dielectric interface that the PRPs are initially sitting on. As we suggested, some may have more surface contact with the SiO_2, or they may have high dielectric local contaminants, thus reducing the amount of the initial shift when covered by the 1.44 oil. After washing in the manner described, we find that successive spectra taken in progressively higher index oils, such as those shown in Figure 2A, display an incremental red shift, which is very regular. We suggest that, once immersed in any of the index oils, the particles are in a more uniform medium with similar dielectric below and above, thereby resulting in a more predictable and regular incremental index and spectral shift. In Figure 2B we have plotted the peak plasmon resonance wavelength versus the index oil value for all of the blue particles studied. It is evident that there is a roughly linear relationship between the local index and the plasmon resonance peak of each particle. Based on the average of linear fits to each of these data sets, we have determined the average red shift fo the blue particles to be 1.6 nm (varying from 1 to 2 nm for the 12 particles studied) per a change of 0.01 in index.

Mie theory for a spherical silver nanoparticle predicts a linear relationship between the dielectric of the medium and the peak plasmon resonance. Malinsky et al. (ref 21, Figure 10A) have calculated that for a 60 nm diameter particle surrounded by a uniform dielectric medium the peak plasmon resonance wavelength will shift 2.1 nm per 0.01 index change. This is a little higher than the average 1.6 nm per 0.01 index change that we found experimentally but, unlike the theory, our particles are sitting on a SiO_2 ($n = 1.56$) dielectric medium, and we expect the proximity of the SiO_2 to cause a reduction in the sensitivity of the plasmon resonance peak to changes of the index of the covering oil. This reduction is illustrated by the calculated red shifts for a 60 nm sphere pre-embedded in a dielectric shell (2 nm thick, $n = 1.42$) prior to changing the surrounding dielectric (ref 21, Figure 10B), which predicts a 1.68 nm per 0.01 change in index. Although this is not an accurate representation of our nanoparticle sitting on SiO_2, the comparison reassures us that the experimental data closely resemble predictions made by Mie theory for similar systems.

The nature (but not the values) of the shift of the plasmon resonance with external index can be analyzed via an electrostatic model when the wavelength is much larger than the particle dimensions. The induced dipole moment for a particle of arbitrary shape embedded in a uniform index has the general form[24]

$$P \sim \frac{\epsilon(\lambda) - \epsilon_{\mathrm{med}}}{\epsilon_{\mathrm{med}} + d(\epsilon(\lambda) - \epsilon_{\mathrm{med}})} \tag{1}$$

In eq 1, d is the depolarization factor. Plasmon resonances occur for those values of $\epsilon(\lambda)$ for which the denominator of eq 1 vanishes, or when

$$\epsilon(\lambda) = \left(1 - \frac{1}{d}\right)\epsilon_{\mathrm{med}} \equiv -\beta\epsilon_{\mathrm{med}} \tag{2}$$

For a sphere, only pure dipole resonances couple to the field, and the depolarization factor is $d = 1/3$; this value of d leads to the familiar condition that a surface plasmon resonance occurs when $\epsilon(\lambda) = -2\epsilon_{\mathrm{m}}$. Differentiating eq 2, using the depolarization factor for a sphere, and the relation $n_{\mathrm{med}}^2 = \epsilon_{\mathrm{med}}$, we find

$$\frac{\mathrm{d}\epsilon(\lambda)}{\mathrm{d}\lambda_r} = -2\frac{\mathrm{d}\epsilon_{\mathrm{med}}}{\mathrm{d}\lambda_r} = -4\frac{\mathrm{d}n_{\mathrm{med}}}{\mathrm{d}\lambda_r} \tag{3}$$

With published values for the $\epsilon(\lambda)$ of silver[29] used to determine the derivative on the left-hand side of eq 3, we would expect a change in resonant frequency with index shift of roughly 0.7 nm per change in index of 0.01, near a wavelength of 500 nm. This is considerably smaller than what was observed; however, the lack of agreement is not surprising, given that effects due to retardation, including radiative damping, become significant for particles of this size.

The visible color of red-shifted red (triangular) particles is dominated by a secondary peak (q′) in the 1.44 and higher index oils, as shown in Figure 1E. Previous work on nanoparticles of similar morphology has shown that this peak likely corresponds to a higher order mode, identified as a quadrupole in reference.[27] We will adopt this term here. Because the quadrupole peak appeared within an optical range convenient for us to study with our apparatus, we performed a similar study on the behavior of this resonance peak as a function of the surrounding index. The quadrupole peak is shifted by an average of 48 nm (varying from 33 to 60 nm for the 10 particles studied) upon application of the 1.44 index oil. As successively higher index oils are applied to the sample, the plasmon resonance peak displays an incremental red shift, as shown in Figure 3A, though by an amount less than that of the dipole plasmon resonance peak of the blue particles. Peak plasmon resonance vs index of oil is plotted in Figure 3B. Based on the average of linear fits to each of these data sets, we have determined the average shift for the quadrupole mode of the red particles is 1.2 nm (varying from 0.6 nm to 1.77 nm for the 10 particles studied) per a change of 0.01 in index of the surrounding medium. This red shift is ∼3/4 that of the blue particle dipole plasmon resonance red shift.

Although we find that the electrostatic theory significantly underestimates the shift of the plasmon resonance wavelength for a changing dielectric, it is useful for understanding the relationship between the dipole and the quadrupole resonance modes. A reduced sensitivity to changes in external index for the resonance wavelength for a quadrupole mode might be expected on the basis of the electrostatic model. The condition for a quadrupole resonance can be determined from eq 2, using $\beta = 3/2$ [ref 30] rather than $\beta = 2$, which would suggest the quadrupole resonance wavelength shift would be three-quarters that of a dipole resonance. This estimate is consistent with the observed relative shifts between the dipole and quadrupole modes; however, this comparison is based entirely on spherical particles and may not be directly applicable to the triangular particles studied here.

Because the dipole plasmon resonance of the red (triangular) particles is shifted out of the visible spectrum as the index of the surrounding medium is raised beyond 1.44, we were generally unable to study the spectra under successively higher index oils. The spectral detection capabilities of our instrument taper off above 800 nm. However, for some of the red particles studied which had an initial plasmon resonant peak less than ∼680 nm, we were able to acquire spectra of the particles covered by 1.44 and 1.48 index oils. An example of the dipole plasmon resonance spectra from one of the red particles is shown in Figure 4. We found that the average initial shift of the dipole resonance from air into the 1.44 oil was 94 nm (varying from 83 to 110 nm for 8 red particles studied). This suggests a greater sensitivity to the change in index than the blue (spherical) particles, which on average shifted only 52 nm from air into the 1.44 index oil. Furthermore, the average shift from 1.44 index oil to 1.48 index oil was 14 nm (varying from 10 nm to 23 nm for 4 red particles), which would correspond to a 3.5 nm per 0.01 index increase. Clearly, there is a greater shift for the red (triangular) particle dipole plasmon resonance than either the blue (spherical) particle dipole plasmon resonance or the quadrupole resonance of the red (triangular) particles. Based on these observations, it is evident that a biosensor based on the detection of the plasmon resonance peak shift would have greater sensitivity using triangular shaped nanoparticles, rather than spherical ones; however, the extent of the difference will, of course, depend strongly on the dispersive properties of the dielectric function.

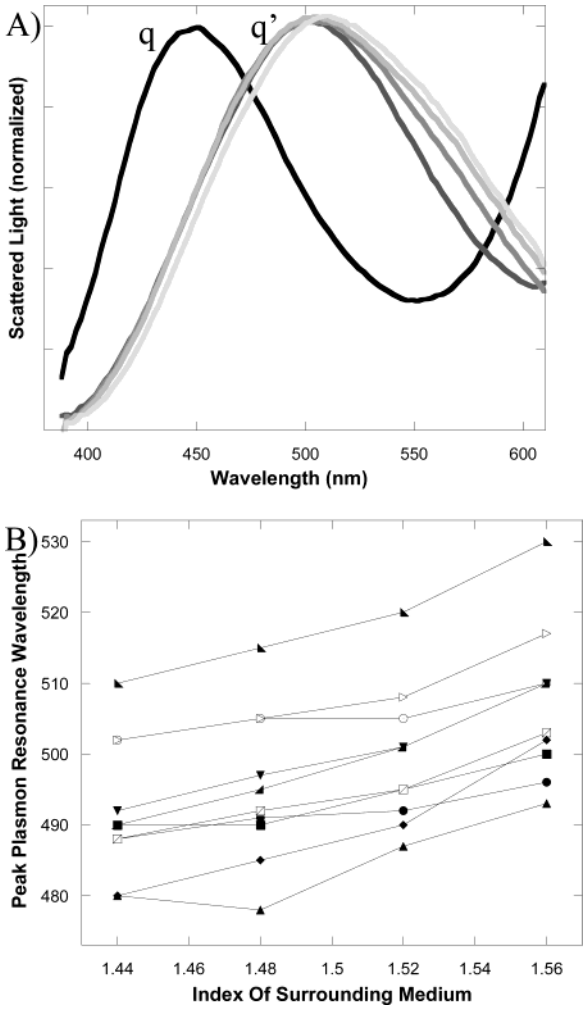

Figure 3. Spectral shift data for quadrupole resonance of individual red (triangular) silver nanoparticles. (A) Typical red particle quadrupole spectrum as it is shifted from (q) air to (q′) 1.44 index oil, and successive oil treatments in 0.04 index incremental increases. (B) Peak quadrupole spectral position vs index of oil applied to red (triangular) silver nanoparticles, for 10 individual red (triangle) particles studied. The average slope of the linear fit to these curves suggests a 1.2 nm red shift per 0.01 index increase.

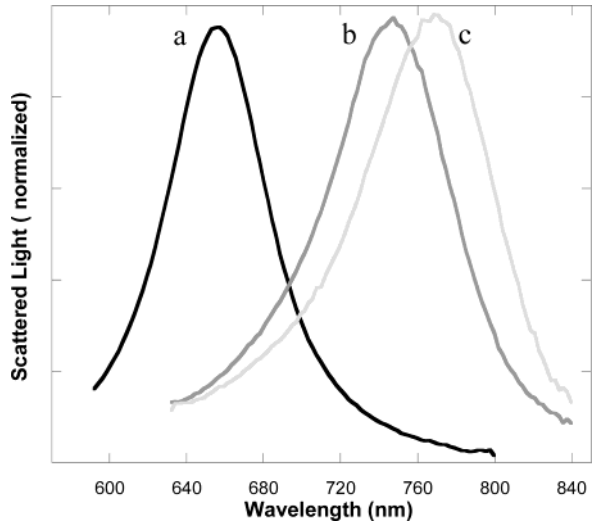

Figure 4. Spectral shift for dipole resonance of typical red (triangular) silver nanoparticle. Spectrum is red shifted from (a) air into (b) 1.44 index oil and further into (c) 1.48 index oil. Further increase in oil index caused the dipole mode spectra to shift out of our detection range for the majority of red (triangle) particles studied. Based on the shift of the dipole resonance of the red particle from 1.44 to 1.48 index oil, for the 4 particles still characterizable over this range, we have determined that the average red shift is 3.5 nm per 0.01 index increase.

In conclusion, we have demonstrated a practical technique for studying the effect of local index on the plasmon resonant scattering spectra of individual silver nanoparticles. The plasmon resonance of each individual silver nanoparticle is highly sensitive to small changes in the local refractive index, which we have systematically characterized. We have also demonstrated that the shape and resonance mode of the nanoparticle affects the sensitivity to these changes. Developing a nanoscale biosensor based on single nanoparticles may be possible, but would be subject to the particle-to-particle variations we have observed affecting the plasmon resonance peak shift from the air/ SiO_2 interface into the more uniform high dielectric medium of the index oils. Rapidly advancing knowledge of the optical properties of individual and collective plasmon resonant nanoparticles of a variety of shapes and configurations under a variety of local environments will enable consideration of a wide variety of applications including but not limited to biosensing.

Acknowledgment. We thank Dr. David Schultz for his help in the initial developments of the techniques described, Steve Oldenburg of Seashell Technology, and Andy Pommer of the UCSD Physics Machine Shop for their valuable technical help. This work was supported by the NIH STTR grant R42 RR 12415.

References

(1) Ditlbacher, H.; Krenn, J. R.; Lamprecht, B.; Leitner, A.; Aussenegg, F. R. Spectrally coded optical data storage by metal nanoparticles. *Opt. Lett.* **2000**, *25*, 563−565.
(2) Quinten, M.; Leitner, A.; Krenn, J. R.; Aussenegg, F. R. Electromagnetic energy transport via linear chains of silver nanoparticles. *Opt. Lett.* **1998**, *23*, 1331.
(3) Ditlbacher, H.; Krenn, J. R.; Schider, G.; Leitner, A.; Aussenegg, F. R. Two-dimensional optics with surface plasmon polaritons. *APL* **2002**, *81*, 1762−1764.
(4) Chicanne, C.; David, T.; Quidant, R.; Weeber, J. C.; Lacroute, Y.; Bourillot, E.; Dereux, A.; Colas des Francs, G.; Girard, C. Imaging the Local Density of States of Optic Corals. *Phys. Rev. Lett.* **2002**, *88*, 097402−1.
(5) Maier, S. A.; Kik, P. G.; Atwater, H. A. Observation of coupled plasmon-polariton modes in Au nanoparticle chain waveguides of different lengths: Estimation of waveguide loss. *Appl. Phys. Lett.* **2002**, *81*, 1714−1716.
(6) Mock, J. J.; Barbic, M.; Smith, D.; Schultz, D.; Schultz, S. 2002. Shape Effects in Plasmon Resonance of Individual Colloidal Silver Nanoparticles. *J. Chem. Phys*. **2002**, *116*(15), 6755−6759.
(7) Sönnichsen, C.; Franzl, T.; Wilk, T.; von Plessen, G.; Feldmann, J. Drastic Reduction of Plasmon Damping in Gold Nanorods. *Phys. Rev. Lett.* **2002**, *88*, 77402−1.
(8) Tamaru, H.; Kuwata, H.; Miyazaki, H. T.; Miyano, K. Resonant light scattering from individual Ag nanoparticles and particle pairs. *APL* **2002**, *80*(10), 1826−1828.
(9) Chen, S.; Carroll, D. L. Synthesis and Characterization of Truncated Triangular Silver Nanoplates. *Nano Lett.* **2002**, *2*, 1003−1007.
(10) Pastoriza-Santos, I.; Liz-Marzan, L. M. Synthesis of Silver Nanoprisms in DMF. *Nano Lett.* **2002**, *2*, 903−905.
(11) Mallin, M. P.; Murphy, C. J. Solution-Phase Synthesis of Sub-10 nm Au−Ag Alloy Nanoparticles. *Nano Lett.* **2002**, *2*, 1235−1237.
(12) Krenn, J. R.; Schider, G.; Rechberger, W.; Lamprecht, B.; Leitner, A.; Aussenegg, F. R. Design of multipolar plasmon excitations in silver nanoparticles. *APL* **2000**, *77*, 3379−3381.
(13) Gotschy, W.; Vonmetz, K.; Leitner, A.; Aussenegg, F. R. Optical dichroism of lithographically designed silver nanoparticle films. *Opt. Lett.* **1996**, *21*(15), 1099−1101.
(14) Schultz, S.; Smith, D. R.; Mock, J. J.; Schultz, D. A. Single molecule detection with nonbleaching multicolor optical immunolabels. *Proc. Natl. Acad. Sci. U.S.A.* **2000**, *97*(3), 996−1001.
(15) www.geniconsciences.com.
(16) Homola, J.; Yee, S. S.; Gauglitz, G. Surface plasmon resonance sensors: review. *Sens. Actuators, B* **1999**, *54*, 3−15.
(17) Nath, N.; Chilkoti, A. A Colorimetric Gold Nanoparticle Sensor to Interrogate Biomolecular Interactions in Real Time on a Surface. *Anal. Chem.* **2002**, *74*, 504−509.
(18) Okamoto, T.; Yamaguchi, I.; Kobayashi, T. Local plasmon sensor with gold colloid monolayers deposited upon glass substrates. *Opt. Lett.* **2000**, *25*(6), 372−374.
(19) Kalyuzhny, G.; Schneeweiss, M. A.; Shanzer, A.; Vaskevich, A.; Rubinstein, I. Differential Plasmon Spectroscopy as a Tool for Monitoring Molecular Binding to Ultrathin Gold Films. *J. Am. Chem. Soc.* **2001**, *123*, 3177−3178.
(20) Haes, A. J.; Van Duyne, R. P. A Nanoscale Optical Biosensor: Sensitivity and Selectivity of an Approach Based on the Localized Surface Plasmon Resonance Spectroscopy of Triangular Silver Nanoparticles. *J. Am. Chem. Soc.* **2002**, *124*, 10596−10604.
(21) Malinsky, M. D.; Kelly, K. L; Schatz, G. C.; Van Duyne, R. P.; Chain Length Dependence and Sensing Capabilities of the Localized Surface Plasmon Resonance of Silver Nanoparticles Chemically Modified with Alkanethiol Self-Assembled Monolayers. *J. Am. Chem. Soc.* **2000**, *123*, 1471−1482.
(22) Jensen, T. R.; Malinsky, M. D.; Kelly, L.; Lazarides, A. A.; Schatz, G. C.; Van Duyne, R. P.; Nanosphere Lithography: Effect of the External Dielectric Medium on the Surface Plasmon Resonance of a Periodic Array of Silver Nanoparticles. *J. Phys. Chem. B* **1999**, *103*, 9846−9853.
(23) Mock, J. J.; Oldenburg, S. J.; Smith, D. R.; Schultz, D. A.; Schultz, S.; Composite Plasmon Resonant Nanowires. *Nano Lett.* **2002**, *2*, 465−469.
(24) Sonnichsen, C.; Geier, S.; Hecker, N. E.; von Plessen, G.; Feldmann, J.; Ditlbacher, H.; Lamprecht, B.; Krenn, J. R.; Aussenegg, F. R.; Chan, V. Z−H.; Spatz, J. P.; Moller, M. Spectroscopy of single metallic nanoparticles using total internal reflection microscopy. *APL* **2000**, *77*, 2949−2951.
(25) Silva, T. J. *Thesis University of California San Diego*, 1994.
(26) Kottman, J. D.; Martin, O. J. F.; Smith, D. R.; Schultz, S. Scattering properties of nanoparticles with arbitrary shape. *Chem. Phys. Lett.* **2001**, *341*, 1−3.

(27) Rongchao, J.; Yun-Wei, C.; Mirkin, C. A.; Kelly, K. L.; Schatz, G. C.; Zheng, J. G. Photoinduced Conversion of Silver Nanospheres to Nanoprisms. *Science* **2001**, *294*, 1901−1903.
(28) Barbic, M.; Mock, J. J.; Schultz, S. Single-Crystal Silver Nanowires Prepared by the Metal Amplification Methodology. *J. Appl. Phys.* **2002**, *91*(11), 9341−9345.
(29) Johnson, P. B.; Christy, R. W. *Phys. Rev. B* **1972**, *6*, 4370.
(30) Kelly, L. K.; Coronado, E.; Zhao, L.-L.; Schatz, G C. The Optical Properties of Metal Nanoparticles. *J. Phys. Chem. B* **2003**, *107*(3), 668−677.

NL0340475